

# Measuring Topological Constraint Relaxation in Ring-Linear Polymer Blends

Daniel L. Vigil,<sup>1</sup> Ting Ge,<sup>2</sup> Michael Rubinstein,<sup>3</sup> Thomas C. O'Connor,<sup>4</sup> and Gary S. Grest<sup>1</sup>

<sup>1</sup>*Sandia National Laboratories, Albuquerque, NM 87185, USA*

<sup>2</sup>*Department of Chemistry and Biochemistry, University of South Carolina, Columbia, South Carolina 29208, USA*

<sup>3</sup>*Department of Mechanical Engineering and Materials Science, Duke University, Durham, North Carolina 27708, USA and*

<sup>4</sup>*Department of Materials Science and Engineering, Carnegie Mellon University, Pittsburgh, Pennsylvania 15213*

(Dated: April 25, 2024)

Polymers are an effective test-bed for studying topological constraints in condensed matter due to a wide array of synthetically-available chain topologies. When linear and ring polymers are blended together, emergent rheological properties are observed as the blend can be more viscous than either of the individual components. This emergent behavior arises since ring-linear blends can form long-lived topological constraints as the linear polymers thread the ring polymers. Here, we demonstrate how the Gauss linking integral can be used to efficiently evaluate the relaxation of topological constraints in ring-linear polymer blends. For majority-linear blends, the relaxation rate of topological constraints depends primarily on reptation of the linear polymers, resulting in the diffusive time  $\tau_{d,R}$  for rings of length  $N_R$  blended with linear chains of length  $N_L$  to scale as  $\tau_{d,R} \sim N_R^2 N_L^{3.4}$ .

Topological constraints are long-lived interactions between atomic degrees of freedom that arise from the entanglement of some element of their phase spaces. They drive a variety of exotic nonlinear dynamics across an array of fields: stabilizing solitons in nonlinear optics [1, 2], hydrodynamic vortices in both classical [3–5] and quantum fluids [6], and fractional electronic states in topological insulators and quantum spin liquids. For most of these systems, the origin of the topological entanglement is subtle and difficult to visualize or characterize directly. The dynamics of polymer melts and blends are also dominated by topological entanglement, but unlike many quantum systems, this entanglement arises from the interweaving, threading, and knotting of the polymer chains in real space. Additionally, the mathematical structure of models of polymer melts is nearly identical to that for many quantum systems [7, 8], so much so that some quantum problems are simulated using ring polymers [9]. In addition, polymers have the advantage of a large body of synthetic and characterization data compared to many other fields due to advances that allow for synthesis of polymers with nearly arbitrary size and chain topology. This makes entangled polymer melts an ideal and economical test bed for exploring the dynamics of systems with complex topological constraints.

For melts of linear polymers, there are mature techniques to evaluate topological constraints. These include contour reduction algorithms [10, 11] and isoconfigurational averaging [12]. Topological constraints in ring polymers, in contrast, have been more difficult to measure. Additionally, recent studies have found that neat ring polymers have significantly different rheological properties from linear polymers due to the differences in knotting and entanglement [13–20]. When ring and linear polymers are blended together, emergent rheological properties are observed as the blend can be more viscous than either of the individual components [21–

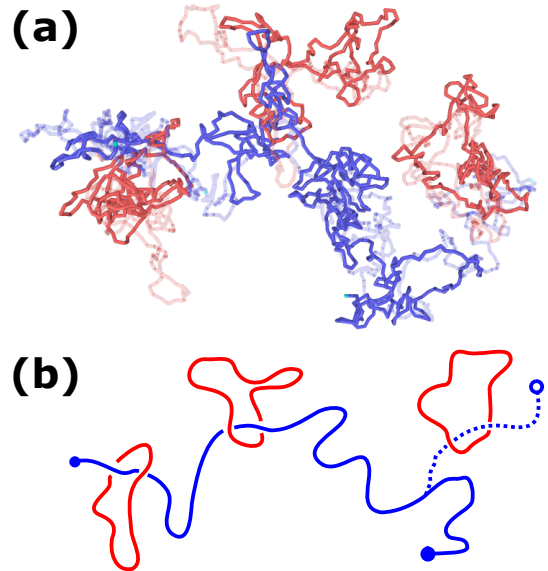


FIG. 1. (a) Snapshot of three ring polymers (red,  $N_R = 200$ ) threaded by a linear polymer (blue,  $N_L = 600$ ) from a molecular dynamics simulation. The initial configuration is faded and the final configuration is shown in bold. In the final configuration, the right ring is no longer threaded. (b) Drawing of the dethreading of the right ring polymer due to motion of the linear chain. The initial configuration is shown with a dashed line and the final configuration is shown with the solid line. Chain ends are marked with circles.

23]. This emergent behavior has been ascribed to the fact that ring-linear blends can form topological constraints via linear polymers threading the ring polymer (Fig. 1) and these ring-linear threads are presumed to be long-lived. Thus far, direct observation of the ring-linear threading/dethreading process has been difficult in experiments and simulations. In this work we use re-

cently implemented topology tools to directly measure ring-linear thread relaxation in simulations of ring-linear polymer blends.

We perform coarse-grained molecular dynamics (MD) simulations of polymer melts where individual polymers are modeled by bead-spring chains with FENE bonds and all beads interact via purely repulsive Lennard-Jones interactions characterized by energy  $\epsilon$  and distance  $\sigma$ . Model details are presented in the SI. Linear chains contain  $N_L$  beads and rings contain  $N_R$  beads. All simulations are conducted in cubic cells with periodic boundary conditions at a particle density of  $0.85 m/\sigma^3$ , where  $m$  is the mass of a bead. Unconcatenated ring polymers were constructed according to previously published methods [24] and blends of various ring volume fraction  $\phi_R$  were constructed by removing a bond from some rings to convert them into linear chains. Simulations are conducted with a Langevin thermostat at temperature  $T = \epsilon/k_B$  with damping parameter  $100\tau$  and were time integrated using a velocity-Verlet algorithm with time step  $0.01\tau$ , where  $\tau = \sqrt{m\sigma^2/\epsilon}$  is the Lennard-Jones time. All simulations were conducted using LAMMPS [25]. System sizes and equilibration times are given in the SI; the blends contained up to 960000 particles and were simulated for up to 10 billion time steps ( $10^8\tau$ ).

To evaluate ring-linear threads, we use an approach based on the Gauss linking integral (GLI), which has recently been implemented in a parallel, open-source code TEPPP [26]. As a post-processing step of our simulations, the periodic linking number  $L_P$  (a generalization of the linking number to periodic simulations [27, 28]) is computed between all pairs of ring and linear chains. Any pair of chains with  $|L_P| > 0.5$  is considered threaded. The periodic linking number can take any real value as we do not invoke a closure approximation on the linear chain, unlike previous work [29]. All beads from the linear chain are included in the analysis, unlike previous work which excluded beads that were within one entanglement length  $N_e$  of the chain end [30]. To further characterize the time dependence of threads, we construct a thread correlation function,  $C(t)$ , analogous to the intermittent association correlation function used to study ion associations in solution [31–34]. Details of the linking number calculation, thread cutoff, and correlation function are discussed further in the SI. The number of ring-linear threads has also been counted via other techniques such as primitive path analysis with contact mapping [30], minimal surfaces [24, 35, 36], and persistent homology [37], though most of these authors have not been able to measure the dynamics of threading nor multiple threads.

The dynamics of individual ring and linear polymers are characterized by the diffusion time  $\tau_d$ . Here we define  $\tau_d$  as the time for the mean squared displacement (MSD) of a bead  $g_1(\tau_d) = \langle (\Delta r(\tau_d))^2 \rangle$  to move  $3\langle R_g^2 \rangle$ , where  $R_g$  is the radius of gyration of a chain [38]. An example of the MSD of the center of mass  $g_3(t)$  motion and of a bead  $g_1(t)$  are presented in Fig. 2 for rings of length  $N_R = 400$  in a pure ring melt and in a blend with  $\phi_R = 0.3$  with

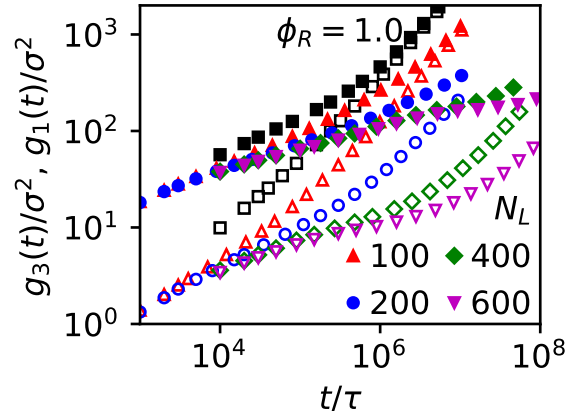


FIG. 2. Mean-squared displacement of ring polymers of length  $N_R = 400$  in pure melts (black squares) or blends with  $\phi_R = 0.3$  (all other symbols). Mean squared displacement of the center of mass  $g_3(t)$  is shown with open symbols and motion of a monomer  $g_1(t)$  with filled symbols.

varying length of the linear chains  $100 \leq N_L \leq 600$ . Fig. 2 clearly shows how as  $N_L$  increases, the ring motion becomes subdiffusive as the rings have to ‘wait’ for the linear chains to release the topological constraints before the ring can relax. While the motion of the rings depends strongly on the length of the linear chains, the motion of the linear is hardly affected by the presence of the rings as shown in Fig. S6.

Theories for chain dynamics in ring-linear blends posit that rings that are threaded by linears cannot diffuse until the topological constraint imposed by the thread is released via linear chain reptation (as seen in the MSD plots). The classical constraint release model assumes that there are  $N_R/N_e$  threads per ring and that the threads are released independently [39]. The time scale for an individual relaxation event scales with the linear chain diffusion time, which scales with the linear chain size as  $\tau_{d,L} \sim N_L^{3.4}$ . The Rouse-like constraint release time for the ring polymer then scales like  $\tau_{d,R} \sim N_R^2 N_L^{3.4}$ . If the linear chains are short, however, there will be a crossover to unentangled ring Rouse relaxation where the diffusion time of the ring scales like  $\tau_{d,R} \sim N_R^2$  and is independent of linear chain size.

The diffusion time for ring polymers in blends with linear polymers of equal chain length  $N_R = N_L = N$  as a function of linear chain length is shown in Fig. 3a. The diffusion time  $\tau_d$  of ring polymers increases as  $N^{5.4}$ , in agreement with theory. In contrast, pure ring polymers have a diffusion time that can be fit to an apparent power law  $\tau_d \sim N_R^{2.8}$  (Fig. 5b) and pure, entangled linear polymers have a diffusion time that scales as  $N_L^{3.4}$  [14].

We next examine the effect of the linear chain size on the relaxation of the rings. We fix the ring size ( $N_R = 200$  or  $N_R = 400$ ) and vary the linear chain length as shown in Fig. 3b. The open symbols show the diffusion time of the

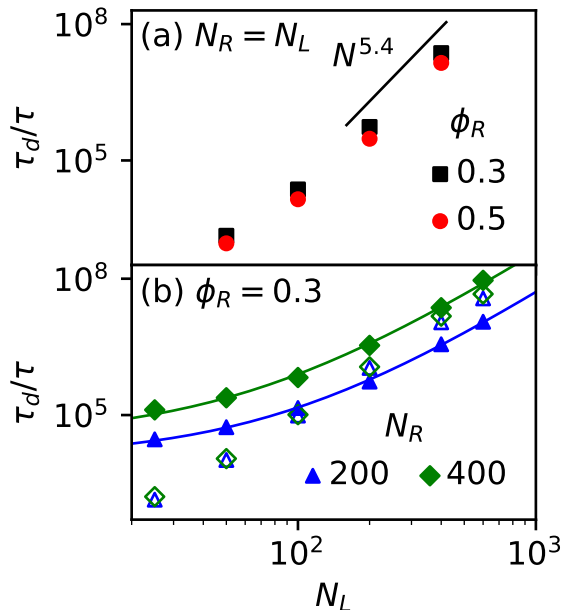


FIG. 3. Diffusion times for ring (filled symbols) and linear polymers (open symbols) versus linear chain length  $N_L$  in a ring-linear blend with (a) equal ring and linear polymer length, (b) fixed ring polymer length and ring fraction  $\phi_R = 0.3$ . Solid lines indicate fitted crossover functions from eq S9.

linear chains, which scales like  $N_L^{3.4}$ , which is expected for entangled linear polymers. For the model considered here, the linear chain entanglement length is  $N_e \approx 28$  [38]. For sufficiently long linear polymers, the ring polymer diffusion time also follows the  $N_L^{3.4}$  scaling. However, for short linear chains, the ring polymer diffusion has a weaker dependence on  $N_L$  and can be fit to a crossover to unentangled ring polymer scaling  $\tau_{d,R} \sim N_L^0$ . The solid lines are a fit to a crossover function (eq S9) that includes the  $N_L^{3.4}$  and  $N_L^0$  limits. The fit indicates a crossover  $N_L$  value around 80.

The thread relaxation  $C(t)$  for blends with  $\phi_R = 0.3$ ,  $N_R = 200$ , and variable  $N_L$  is shown in Fig. 4a.  $C(t)$  shows a similar shape for all  $N_L$ , but with shifted time scales. These data can be collapsed by choosing a value of the correlation function, in this case 0.5, and rescaling time for each curve so that all curves overlap at the chosen value. The time-rescaled data is given in Fig. 4b and the inset shows the times  $\tau_{0.5}$  used to collapse all the data versus the diffusion time  $\tau_{d,L}$  of the linear chains. The  $C(t)$  curves collapse nearly perfectly onto each other, indicating that the dethreading dynamics is similar with increasing linear polymer size.

The inset shows that  $\tau_{0.5}$  is directly proportional to the linear chain diffusion time, though it is smaller by a factor of  $\approx 1/6$  for blends with  $\phi_R = 0.3$  and  $N_R = 200$ . To relax the thread only requires a portion of the linear chain to reptate through the ring, so it is expected for the dethreading time to be less than the diffusion time.

We now evaluate the effect of the ring polymer size on the chain diffusion and dethreading. When varying  $N_R$  one must be careful to note that small rings and large rings in pure ring melts have different scaling behavior. In pure ring melts, small rings are almost unperturbed Gaussian rings with size that scales like  $R_g^2 \sim N$ . As the size of the ring increases, the rings impinge on each other and there is a crossover to a loopy globule scaling regime where  $R_g^2 \sim N^{2/3}$  [40]. Rings in ring/linear blends are expected to follow  $R_g^2 \sim N_R$  if the rings are sufficiently diluted by linears. If a critical ring concentration is exceeded in the blend, then the large ring scaling  $R_g^2 \sim N_R^{2/3}$  will be recovered. The critical concentration is a function of the ring size, so increasing ring polymer size at fixed volume fraction of rings may cause one to cross the critical concentration.

Fig. 5a shows the mean squared radius of gyration of ring polymers in ring-linear blends ( $\phi_R = 0.3$  and  $\phi_R = 0.5$ ) and pure ring melts ( $\phi_R = 1.0$ ) versus the size of the rings  $N_R$ . The linear chains have length  $N_L = 200$  in the blends. The data in Fig. 5a were fit to a crossover function (eq S10) and a crossover  $N_R$  was extracted for the blends and the pure rings. For blend systems the crossover occurs for  $N_R = 445$  ( $\phi_R = 0.3$ ) or  $N_R = 328$  ( $\phi_R = 0.5$ ), so most of the data lies in the dilute-ring scaling regime. For the pure ring melts ( $\phi_R = 1$ ) the crossover occurs for  $N_R = 122$ , so most of the data lies in the concentrated ring regime.

The diffusion times for ring polymers are shown in Fig. 5b. For rings that are of similar size to the linear chains ( $100 \leq N_R \leq 400$ ), the ring diffusion time in the blends (red and black points) is an order of magnitude larger than in the pure melt ring (blue points). In this regime the ring motion is dominated by ring-linear threadings, which are slow to relax. For small rings ( $N_R \leq 50$ ) the diffusion times in blends is much closer to the diffusion time in the pure ring melt. This is because the rings are so small that they have zero to two threads (Fig. 6a), and thus have few topological constraints to slow them down compared to the pure ring melt. For larger rings ( $N_R \geq 800$ ), the blend and pure melt diffusion times also approach in value. In this regime, the ring dynamics are also affected by ring-ring interactions which are similar between blends and pure ring melts.

The number fraction of rings with a given number of linear chains threading the ring,  $N_t$ , is shown in Fig. 6a. The solid points show the value measured in MD simulations via the GLI analysis. Open symbols indicate a Poisson distribution with mean equal to that of the MD results. For the smallest ring size  $N_R = 50$ , the majority of rings have two or fewer linear chains threading them at all. As the ring size  $N_R$  is increased, the distribution of number of threads broadens and moves to larger mean values, consistent with previous investigations [29, 36]. Notably the Poisson distribution fits the measured distribution well for all  $N_R$ . This may indicate that ring-linear threads are independent of each other.

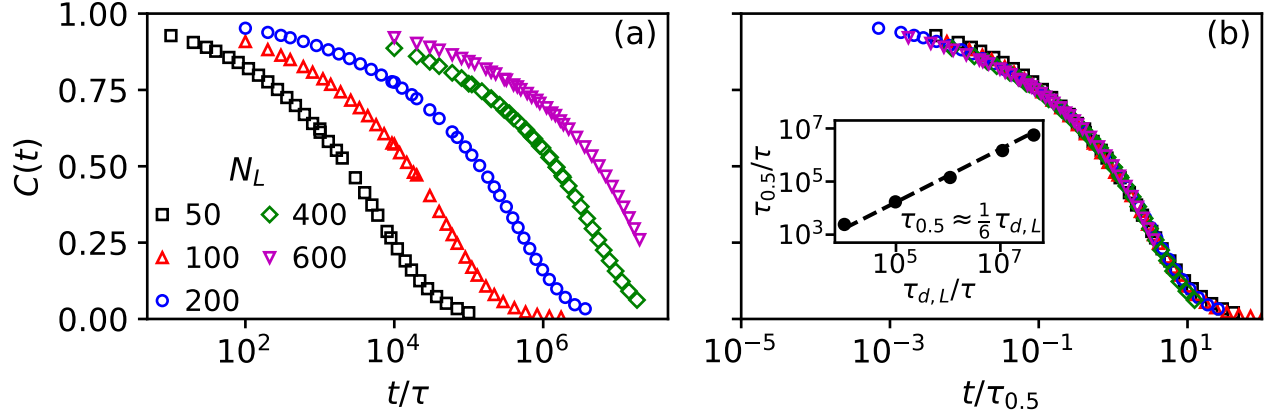


FIG. 4. (a) Dethreading correlation function  $C(t)$  for a ring-linear blend with ring fraction  $\phi_R = 0.3$  and ring length  $N_R = 200$ . (b)  $C(t)$  versus  $t/\tau_{0.5}$ , where  $\tau_{0.5}$  is the time at which only 50% of the original ring-linear threads remain, which is different for each linear length. The inset shows the thread relaxation time scale  $\tau_{0.5}$  versus the diffusion time for a linear chain,  $\tau_{d,L}$ .

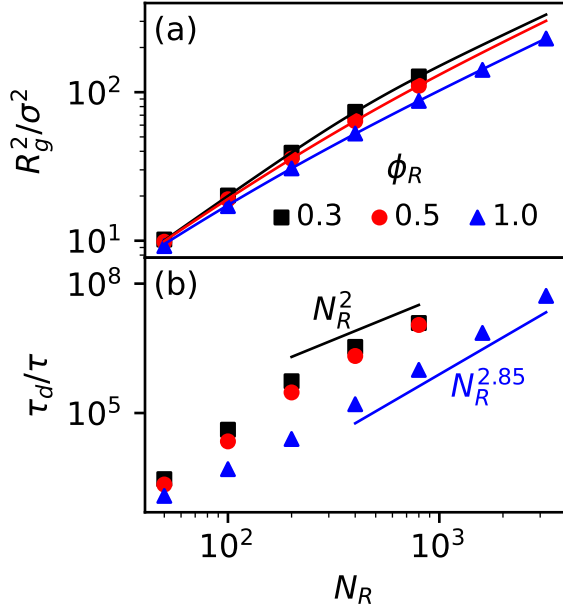


FIG. 5. (a) Radius of gyration  $R_g$  and (b) diffusion time  $\tau_d$  for ring polymers versus ring chain length  $N_R$  in a ring-linear blends and a pure ring melt. In the blends, the linear chain length  $N_L = 200$ . Solid lines in part (a) indicate fit to crossover functions given in eq S10.

The inset of Fig. 6a shows the average number of linear chains threading a ring,  $\bar{N}_t$ , versus the ring size  $N_R$ . The average number of linears threading a ring increases linearly with the ring size,  $\bar{N}_t \sim N_R$ , which is consistent with previous results based on primitive path analysis [30] and minimal surfaces [36].

The dethreading correlation function for the blends

with  $\phi_R = 0.3$  is shown in Fig. 6b. For times  $t/\tau < 10^5$  the curves overlap. Note that no rescaling of time has been performed, unlike in Fig. 4b. The overlapped curves indicate that dethreading dynamics at short times is largely independent of ring size. This indicates that it is the motion of the linear that largely drives dethreading, consistent with previous work.

At long times,  $C(t)$  decays to zero more quickly for smaller rings whereas larger rings have a slow relaxing component that gets slower with increasing ring size. The universal functional form that was observed for linear polymers of different sizes in the blends does not occur for rings. Thus, blending ring and linear polymers has an asymmetric effect where thread relaxation has some complicated dependence on ring polymer size and diffusion, but for linear chains depends only on the diffusion time.

## ACKNOWLEDGMENTS

D.L.V. acknowledges useful discussion with Eleni Panagiotou, the author of the TEPPP software. T.G. acknowledges start-up funds from the University of South Carolina. T.O. acknowledges start-up funds from Carnegie Mellon University. M. R. acknowledges financial support from the National Institutes of Health under Grant P01-HL164320. This work was supported in part by the National Science Foundation EPSCoR Program under NSF Grant Np. OIA-1655740. Any opinions, findings, and conclusions, or recommendations expressed in this material are those of the authors and do not necessarily reflect those of the National Science Foundation. This work was performed, in part, at the Center for Integrated Nanotechnologies, an Office of Science User Facility operated for the U.S. Department of Energy (DOE) Of-

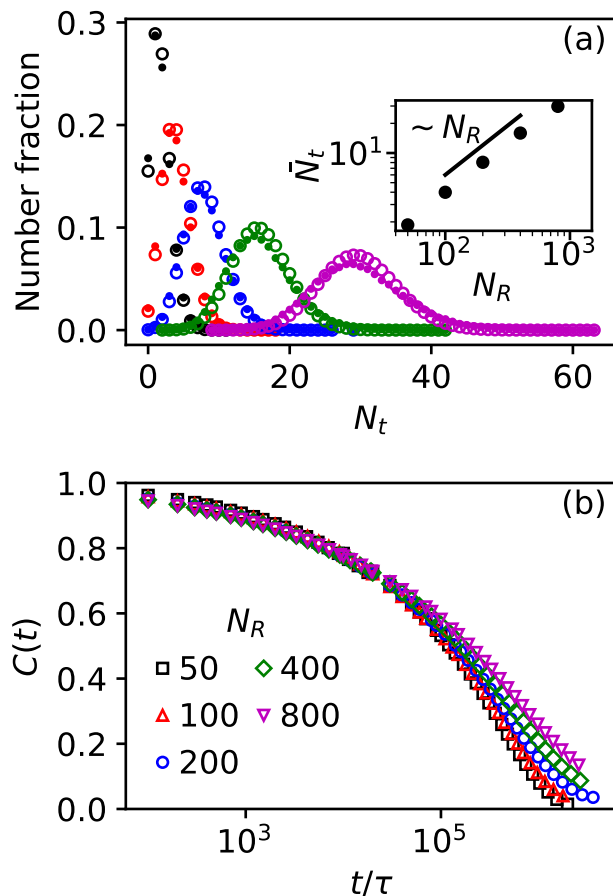


FIG. 6. (a) Number fraction of ring polymers with a given number of linear polymers threading the ring,  $N_t$ . Linear polymers have length  $N_L = 200$  and  $\phi_R = 0.3$ . Solid dots indicate results from MD simulations. Open symbols indicate a Poisson distribution with identical mean to the MD results. Inset shows the average number of linear chains threading the ring  $\bar{N}_t$  versus ring polymer size  $N_R$ . (b) Dethreading correlation function  $C(t)$  versus time  $t$  for the same blends as in (a).

fice of Science. Sandia National Laboratories is a multi-mission laboratory managed and operated by National Technology & Engineering Solutions of Sandia, LLC, a wholly owned subsidiary of Honeywell International, Inc., for the U.S. DOE's National Nuclear Security Administration under Contract No. DE-NA-0003525. The views expressed in the Letter do not necessarily represent the views of the U.S. DOE or the U.S. Government.

- 
- [1] J. Leach, M. R. Dennis, J. Courtial, and M. J. Padgett, *Nature* **432**, 165 (2004).
  - [2] W. T. M. Irvine, *J. Phys. A Math. Theor.* **43**, 385203 (2010).
  - [3] W. Thomson, *Trans. Royal Soc. Edinburgh* **25**, 217–260 (1868).
  - [4] W. Thomson, *Proc. Royal Soc. Edinburgh* **6**, 94–105 (1869).
  - [5] D. Kleckner and W. T. M. Irvine, *Nature Physics* **9**, 253 (2013).
  - [6] D. Proment, M. Onorato, and C. F. Barenghi, *Phys. Rev. E* **85**, 036306 (2012).
  - [7] D. Chandler and P. G. Wolynes, *J. Chem. Phys.* **74**, 4078 (1981), <https://pubs.aip.org/aip/jcp/article-pdf/74/7/4078/11047200/4078.1.online.pdf>.
  - [8] G. H. Fredrickson and K. T. Delaney, *Field-Theoretic Simulations in Soft Matter and Quantum Fluids*, Vol. 173 (Oxford University Press, Incorporated, Oxford, 2023).
  - [9] I. R. Craig and D. E. Manolopoulos, *J. Chem. Phys.* **121**, 3368 (2004), <https://pubs.aip.org/aip/jcp/article-pdf/121/8/3368/10863334/3368.1.online.pdf>.
  - [10] S. K. Sukumaran, G. S. Grest, K. Kremer, and R. Everaers, *J. Polymer Science Part B: Polymer Physics* **43**, 917 (2005).
  - [11] C. Tzoumanekas and D. N. Theodorou, *Macromolecules* **39**, 4592 (2006).
  - [12] W. Bisbee, J. Qin, and S. T. Milner, *Macromolecules* **44**, 8972 (2011), <https://doi.org/10.1021/ma2012333>.

- [13] K. Koniaris and M. Muthukumar, *J. Chem. Phys.* **95**, 2873 (1991).
- [14] J. D. Halverson, W. B. Lee, G. S. Grest, Y. A. Grosberg, and K. Kremer, *J. Chem. Phys.* **134**, 204905 (2011).
- [15] Y. Doi, K. Matsubara, Y. Ohta, T. Nakano, D. Kawaguchi, Y. Takahashi, A. Takano, and Y. Matsushita, *Macromolecules* **48**, 3140 (2015).
- [16] T. Ge, S. Panyukov, and M. Rubinstein, *Macromolecules* **49**, 708 (2016).
- [17] D. Parisi, S. Costanzo, Y. Jeong, J. Ahn, T. Chang, D. Vlassopoulos, J. D. Halverson, K. Kremer, T. Ge, M. Rubinstein, *et al.*, *Macromolecules* **54**, 2811 (2021).
- [18] M. A. Ubertini, J. Smrek, and A. Rosa, *Macromolecules* **55**, 10723 (2022).
- [19] M. Q. Tu, O. Davydovich, B. Mei, P. K. Singh, G. S. Grest, K. S. Schweizer, T. C. O'Connor, and C. M. Schroeder, *ACS Polymers Au* **3**, 307 (2023), <https://doi.org/10.1021/acspolymersau.2c00069>.
- [20] R. Staño, C. N. Likos, and J. Smrek, *Soft Matter* **19**, 17 (2023).
- [21] J. Roovers, *Macromolecules* **21**, 1517 (1988).
- [22] K. R. Peddireddy, M. Lee, C. M. Schroeder, and R. M. Robertson-Anderson, *Phys. Rev. Res.* **2**, 023213 (2020).
- [23] D. Parisi, M. Kaliva, S. Costanzo, Q. Huang, P. J. Lutz, J. Ahn, T. Chang, M. Rubinstein, and D. Vlassopoulos, *Journal of Rheology* **65**, 695 (2021).
- [24] J. Smrek, K. Kremer, and A. Rosa, *ACS Macro Letters* **8**, 155 (2019).
- [25] A. P. Thompson, H. M. Aktulga, R. Berger, D. S. Bolinteanu, W. M. Brown, P. S. Crozier, P. J. in 't Veld, A. Kohlmeyer, S. G. Moore, T. D. Nguyen, R. Shan, M. J. G. J. Tranchida, C. Trott, and S. J. Plimpton, *Comp. Phys. Comm.* **271**, 108171 (2022).
- [26] T. Herschberg, K. Pifer, and E. Panagiotou, *Comp. Phys. Comm.* **286**, 108639 (2023).
- [27] E. Panagiotou, C. Tzoumanekas, S. Lambropoulou, K. C. Millett, and D. N. Theodorou, *Prog. Theor. Phys. Supp.* **191**, 172 (2011), <https://academic.oup.com/ptps/article-pdf/doi/10.1143/PTPS.191.172/5311699/191-172.pdf>.
- [28] E. Panagiotou, *J. Comp. Phys.* **300**, 533 (2015).
- [29] K. Hagita and T. Murashima, *Polymer* **218**, 123493 (2021).
- [30] T. C. O'Connor, T. Ge, and G. S. Grest, *J. Rheo.* **66**, 49 (2022), <https://pubs.aip.org/sor/jor/article-pdf/66/1/49/16587829/49.1.online.pdf>.
- [31] A. Luzar and D. Chandler, *Phys. Rev. Lett.* **76**, 928 (1996).
- [32] F. Müller-Plathe, *J. Chem. Phys.* **108**, 8252 (1998).
- [33] A. Chandra, *Phys. Rev. Lett.* **85**, 768 (2000).
- [34] W. Zhao, F. Leroy, B. Heggen, S. Zahn, B. Kirchner, S. Balasubramanian, and F. Müller-Plathe, *J. Am. Chem. Soc.* **131**, 15825 (2009).
- [35] J. Smrek and A. Y. Grosberg, *ACS Macro Letters* **5**, 750 (2016).
- [36] W. Wang, J. Lu, and R. Sun, *Polymer* **290**, 126513 (2024).
- [37] F. Landuzzi, T. Nakamura, D. Michieletto, and T. Sakaue, *Phys. Rev. Res.* **2**, 033529 (2020).
- [38] H.-P. Hsu and K. Kremer, *J. Chem. Phys.* **144**, 154907 (2016).
- [39] D. Parisi, J. Ahn, T. Chang, D. Vlassopoulos, and M. Rubinstein, *Macromolecules* **53**, 1685 (2020).
- [40] M. Kruteva, J. Allgaier, and D. Richter, *Macromolecules* **56**, 7203 (2023).